Molecular and electronic structure and IR spectra of mononuclear dinitrosyl iron complex $[Fe(SC_2H_3N_3)(SC_2H_2N_3)(NO)_2]$: a theoretical study

A. F. Shestakov, Yu. M. Shul´ga, N. S. Emel´yanova, N. A. Sanina, and S. M. Aldoshin*

Institute of Problems of Chemical Physics, Russian Academy of Sciences, 1 prosp. Akad. Semenova, 142432 Chernogolovka, Moscow Region, Russian Federation. Fax: +7 (496) 515 5420. E-mail: a.s@icp.ac.ru

The molecular and electronic structures of different isomers of a mononuclear dinitrosyl iron complex $[Fe(SC_2H_3N_3)(SC_2H_2N_3)(NO)_2]$ were calculated by the B3LYP and PBE density functional methods. Both theoretical approaches provide good agreement between the calculated and experimental geometry of the lowest-lying isomer (bond lengths differ by 0.02—0.04 Å and bond angles differ by 2—3° in terms of root-mean square values). A feature of the complex is an intramolecular hydrogen bond N—H...N between the thiolate and thione ligands, which causes equalization of the Fe—S and S—C bond lengths. The ground state of the system has a spin of 1/2 and exists at antiparallel orientation of the spin (S = 3/2) of the Fe atom with formal electron configuration d^7 and two local spins (S = 1/2) of the NO ligands. Although each NO group has a small negative charge, which is mainly localized on the O atom, the Fe—NO bond can be treated as similar to homeopolar one. This corresponds to the effective trivalent state of Fe with an oxidation state of 1+. Both theoretical methods correctly reproduce the experimental structure of the IR spectrum, but the PBE functional provides a better description of absolute positions of spectral lines, whereas the B3LYP functional gives a somewhat better description of the relative intensities of spectral components. In spite of similar geometric parameters of coordination of two NO groups, the splitting between the NO stretching bands is rather large (58 cm^{-1}); this value is satisfactorily reproduced in theoretical calculations. A strong intramolecular hydrogen bond causes a large frequency shift of the N—H stretching vibrations corresponding to a broad absorption band in the region 2300—2600 cm^{-1}.

Key words: sulfur-nitrosyl iron complexes, nitrogen monoxide donors, IR spectroscopy, quantum chemical calculations, density functional, B3LYP, PBE, electronic structure.

Dinitrosyl iron complexes with sulfur-containing ligands are biomimetic models for natural donors of nitrogen monoxide.[1] Recently, they have been intensively studied in relation with possible use in medicine as NO donors.[2,3] Mononuclear dinitrosyl iron complexes with sulfur-containing ligands exhibit a characteristic EPR signal with $g \approx 2.03$ in solutions. Only a few crystal structures of this type of complexes are available at the moment.[4—8] To search for new complexes, we proposed to use aza-heterocyclic thiols (in particular, substituted 1,2,4-triazol-3-thiols having a great coordination potential and showing a broad spectrum of biological activities)[9,10] as sulfur-containing ligands. We synthesized a new neutral mononuclear iron complex with 1,2,4-triazol-3-thiolyl ligand and carried out room-temperature[11] and low-temperature[12] X-ray studies of the species. In this work report on a quantum chemical study of the molecular and electronic structures and IR spectra of this complex.

Experimental

Density functional theoretical studies of isolated complex $[Fe_2(SC_2H_3N_3)(SC_2H_2N_3)(NO)_2]$ (**1**) and its possible isomers were carried out by the B3LYP method with the 6-31G* basis set and the GAUSSIAN-98 program[13] and by the PBE method with the SBK pseudopotential and an extended basis set using the PRIRODA program (see Ref. 14). The energies of the optimized structures were compared with inclusion of zero-point vibrational energies. The B3LYP calculated total energies were obtained using the 6-311++G** basis set. IR spectra of complex **1** synthesized following a known procedure[11] were recorded on a Perkin—Elmer/Spectrum BX Fourier-Transform spectrophotometer. Samples were prepared as KBr pellets (1 mg of the compound under study per 300 mg of KBr).

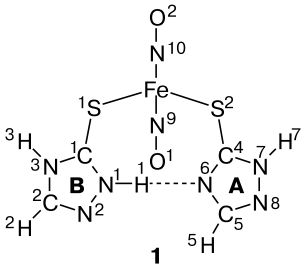

1

Published in Russian in *Izvestiya Akademii Nauk. Seriya Khimicheskaya,* No. 7, pp. 1244—1252, July, 2007.

1066-5285/07/5607-1289

Results and Discussion

Figure 1 shows the optimized structures of complex **1** and its possible isomers. Table 1 lists the calculated bond lengths and bond angles in structure **1a** and, for the sake of comparison, corresponding experimental data for a molecular crystal of composition $[Fe_2(SC_2H_3N_3)(SC_2H_2N_3)(NO)_2]\cdot 0.5H_2O$. The bond lengths ($\delta_R$) and bond angles ($\delta_A$) determined at two temperatures using the sample presented in Table 1 differ (in terms of root-mean square values) by 0.0101 Å and 0.49°, respectively, being no greater than the sum of the corresponding experimental errors in determination. However, comparison of the experimental and theoretical data shows a systematic character of this difference. Compared with the results of B3LYP/6-31G* and PBE/SBK calculations, the δ_R values respectively decrease from 0.037 and 0.022 Å at $T = 283$ K to 0.031 and 0.015 Å at $T = 100$ K. In this case the δ_A values somewhat increase at temperature loweing (from 2.4 and 1.5° at $T = 283$ K to 2.8 and 1.7° at $T = 100$ K for B3LYP and BPE methods correspondingly). By and large, the results of PBE/SBK calculations are in somewhat better agreement with the experimental geometric parameters of the complexes in the crystal. However, the reason for this improvement remains unclear because there are clearly seen systematic differences between the geometry of isolated complex, which is unknown at the moment, and that of the complex in the crystal lattice, as well as errors in calculations.

Formally, the structure of the complex comprises the thiolate (**A**) and thione (**B**) ligands. The thiolate ligand protonated at the sulfur atom and the thione ligand are isomeric forms of 3-mercapto-1,2,4-triazole.

Figure 2 presents the structures of all possible isomeric forms, namely, two thione (**2a**,**d**) and three thiolate ones (**2b**,**c**,**e**) and their relative energies obtained from B3LYP calculations. The isomers differ in position of the mobile hydrogen atom bonded to the nitrogen atom. Structure **2a** has the lowest energy, the isomeric thiol structures with energies of 5.3 (**2b**) and 5.4 (**2c**) kcal mol^{-1} being the next; structures **2d**,**e** lie even much higher on the energy scale. The thione structure **2d** has conjugated double bonds but is nonplanar, which seems to be responsible for the higher energy. Since in alkali media the thiol forms can be ionized with energy gain, both forms of the ligand coexist during the synthesis of the complex, which involves replacement of the negatively charged bridging ligand in the binuclear complex $[Fe_2(NO)_4(\mu\text{-}S_2O_3)_2]^{2-}$.[11]

At the same time the Fe—S(1), Fe—S(2), and S(1)—C(1), S(1)—C(4) bond lengths in the ligands **A** and **B** differ insignificantly, namely, by 0.020 and 0.022 Å (X-ray data), 0.061 and 0.028 Å (B3LYP), and 0.093 and 0.033 Å (PBE). One can assume that this equalization of the ligand structures is, on the one hand, due to the effects of coordination and, on the other hand, to the strong intramolecular hydrogen bond N(1)...H(1)—N(6). (In the case of complete proton transfer the thione and thiolate ligands should exchange their positions.) In addition, there are some weaker intermolecular hydrogen bonds in the crystal structure of complex **1**, which affect the magnitude of the differences between the experimental and theoretical geometry of the complex. In particular, shortening of the C(1)—N(3) bond compared to the ordinary bond seems to be due to the formation of intermolecular hydrogen bond with the N(3)—H(3) fragment.[11] To reveal the effect of the intramolecular hydrogen bond, we calculated the optimum structure of a rotamer of complex **1b** with a weak hydrogen bond S...H instead of the strong hydrogen bond N...H. According to calculations, the energy of the complex is 8.4 (B3LYP) and 7.7 (PBE) kcal mol^{-1} higher than that of the lowest-lying structure **1a**. In this isomer the differences in the Fe—S and S—C bond lengths become nearly doubled, being respectively equal to 0.096 and 0.049 Å (B3LYP) and 0.130 and 0.054 Å (PBE). The results of calculations show that the C—S bond length difference between the isomeric forms of free ligand is twice as large, namely, 0.100 Å (B3LYP/6-31G*). This indicates a pronounced effect of the strong hydrogen bond on equalization of the two ligand structures. According to PBE calculations of the structure with no hydrogen bond (structure **1b**), the SC—N bond lengths in the thione ligand equalize but the difference between the SC—N bonds in the thiolate ligand becomes more pronounced (corresponding differences are 0.029 and 0.011 Å in the starting complex and 0.005 and 0.023 Å in the rotamer). B3LYP calculations gave similar results. The structure of rotamer **1c** with the intramolecular hydrogen bond N(3)—H(3)...N(6) has a somewhat lower energy; however, complexes **1a** and **1c** have considerably different dipole moments (6.6 and 3.9 D, respectively, according to B3LYP/6-311++G** calculations). This large difference should lead to considerable gain in the energy of dipole-dipole interaction in the crystal structure of complex **1a**, which seems to be responsible for the formation of the crystals of complex **1** from molecules **1a** rather than any other isomeric forms.

The isomeric thiols **2b** and **2c** have very similar energies. However, the isomeric complexes **1d** and **1e** with the **2c**-type thiolate ligands lie higher on the energy scale compared to **1a**. Intramolecular hydrogen bonds in these structures are about 0.1 Å longer than in the complexes **1a** and **1b**. One can assume that the reason for differences between them is steric strain in structures **1d**,**e** due to the absence of a plane common to the rings **A** and **B**. This manifests itself in smaller energy expenditure for the formation of structure **1f** *via* cleavage of the strong hydrogen bond N—H...N. Noncoplanarity of the ligands in complexes **1d**,**e** causes the molecular volume to increase and also has a negative effect on the packing energy.

Table 1. Bond lengths (d) and bond angles (ω) in complex **1** determined by different methods*

Parameter	Numerical value					
	I	II	III	IV	V	VI
Bond			d/Å			
Fe—N(9)	1.669(2)	1.6861(6)	1.731	1.670	1.801	1.973
Fe—N(10)	1.677(2)	1.6903(6)	1.735	1.674	1.694	1.717
Fe—S(2)	2.298(1)	2.3015(2))	2.334	2.287	2.287	2.302
Fe—S(1)	2.318(1)	2.3219(2)	2.427	2.347	2.361	2.408
S(2)—C(4)	1.725(2)	1.7308(6)	1.744	1.751	1.734	1.755
S(1)—C(1)	1.703(2)	1.7072(6)	1.711	1.723	1.726	1.725
O(1)—N(9)	1.157(3)	1.1641(8)	1.180	1.178	1.194	1.212
O(2)—N(10)	1.150(3)	1.1626(8)	1.179	1.177	1.178	1.181
N(6)—C(4)	1.333(3)	1.3416(8)	1.341	1.348	1.348	1.346
N(6)—C(5)	1.348(3)	1.3561(8)	1.366	1.368	1.368	1.367
N(7)—C(4)	1.334(3)	1.3405(7)	1.352	1.363	1.362	1.362
N(7)—N(8)	1.359(3)	1.3656(7)	1.362	1.363	1.363	1.361
N(8)—C(5)	1.301(3)	1.3190(8)	1.318	1.327	1.327	1.328
N(1)—C(1)	1.322(3)	1.3353(7)	1.341	1.348	1.348	1.348
N(1)—N(2)	1.375(2)	1.3755(7)	1.370	1.372	1.370	1.371
N(3)—C(1)	1.353(3)	1.3590(7)	1.370	1.378	1.377	1.377
N(3)—C(2)	1.343(3)	1.3585(8)	1.372	1.375	1.373	1.374
N(2)—C(2)	1.298(3)	1.3062(7)	1.301	1.310	1.311	1.311
N(1)—N(6)	2.717(3)	2.701(1)	2.694	2.757		
Bond angle			ω/deg			
N(9)—Fe—N(10)	118.7(1)	119.79(3)	115.0	—	117.6	—
N(9)—Fe—S(2)	111.2(1)	110.76(2)	111.3	—	108.6	—
N(10)—Fe—S(2)	103.2(1)	102.74(2)	106.4	—	105.7	—
N(9)—Fe—S(1)	108.1(1)	107.86(2)	108.9	—	108.8	—
N(10)—Fe—S(1)	103.2(1)	103.23(2)	102.7	—	104.3	—
S(2)—Fe—S(1)	112.0(1)	112.297(7)	112.3	—	111.8	—
C(4)—S(2)—Fe	105.2(1)	105.28(2)	104.1	—	105.3	—
C(1)—S(1)—Fe	106.3(1)	106.110(19)	106.9	—	106.1	—
O(1)—N(9)—Fe	168.2(3)	169.02(7)	163.8	—	169.9	—
O(2)—N(10)—Fe	171.5(3)	172.84(6)	162.8	—	167.6	—
C(4)—N(6)—C(5)	103.7(2)	103.98(5)	104.2	—	104.5	—
C(4)—N(7)—N(8)	110.4(2)	110.20(5)	112.0	—	112.1	—
C(5)—N(8)—N(7)	102.7(2)	103.01(5)	101.6	—	101.9	—
C(1)—N(1)—N(2)	111.7(2)	111.57(5)	112.8	—	112.5	—
C(1)—N(3)—C(2)	107.2(2)	107.30(5)	107.9	—	107.9	—
C(2)—N(2)—N(1)	103.6(2)	104.27(5)	104.5	—	105.0	—
N(6)—C(4)—N(7)	108.5(2)	108.78(5)	107.3	—	106.9	—
N(6)—C(4)—S(2)	127.9(2)	127.73(4)	129.7	—	130.0	—
N(7)—C(4)—S(2)	123.6(2)	123.50(4)	123.0	—	123.1	—
N(8)—C(5)—N(6)	114.6(2)	114.02(5)	114.9	—	114.6	—
N(1)—C(1)—N(3)	105.4(2)	105.39(5)	103.9	—	104.0	—
N(1)—C(1)—S(1)	130.8(2)	130.77(4)	131.8	—	131.7	—
N(3)—C(1)—S(1)	123.7(2)	123.73(4)	124.4	—	124.3	—
N(2)—C(2)—N(3)	112.1(2)	111.45(5)	110.9	—	110.6	—
N(1)—H(1)—N(6)	169.2(2)	153.74(2)	173.9	—	174.0	—

* Experimental data obtained at room temperature[11] (I) and at 100 K (see Ref. 12) (II); results of B3LYP/6-31G* calculations (III); and results of PBE/SBK calculations of the doublet (IV), quadruplet (V), and sextet (VI) states.

Analysis of the electronic structure of complex **1** (Table 2) shows that the resulting total spin $S = 1/2$ can be obtained in the case of antiparallel orientation of the spin of the Fe atom ($S = 3/2$) and the spins of the NO ligands ($S = -1/2$ for each ligand). The corresponding spin densities on the atoms and atomic groups are

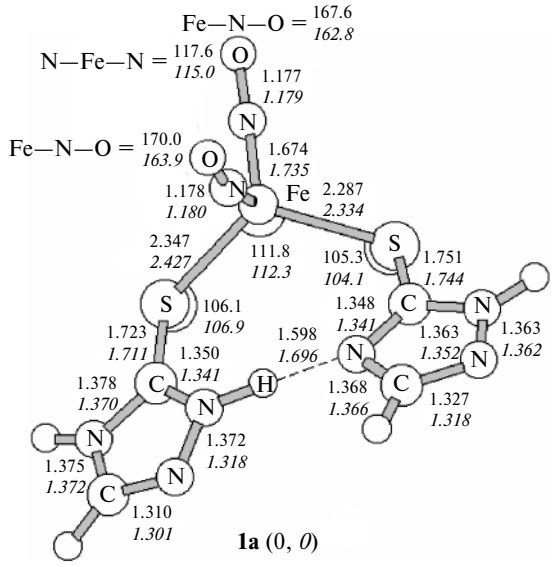

1a (0, *0*)

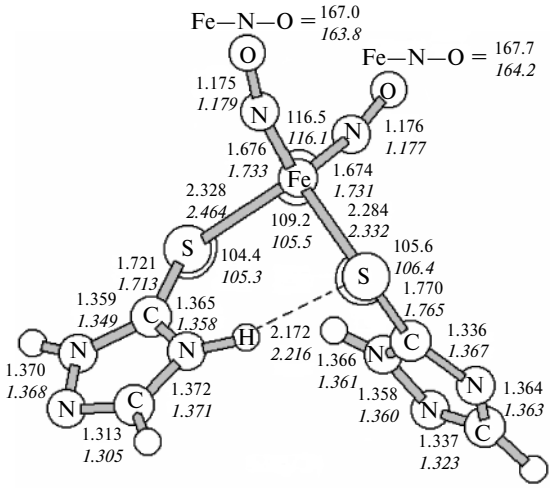

1b (7.7, *8.4*)

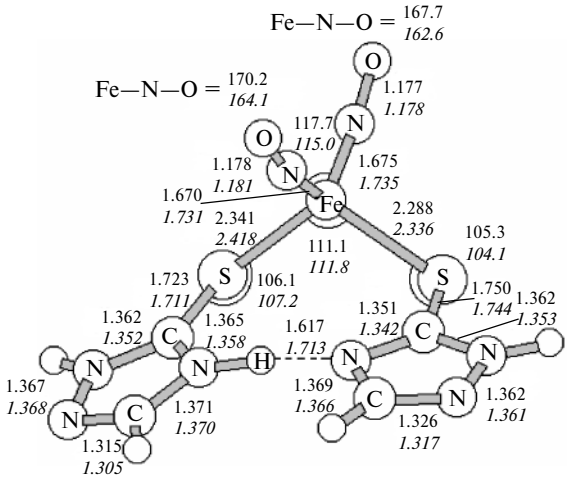

1c (−1.5, *−1.5*)

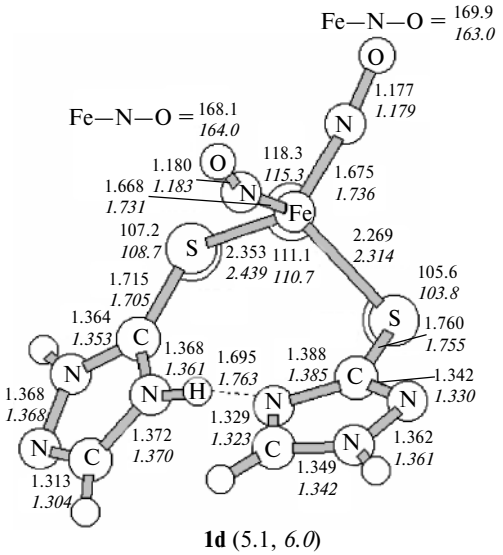

1d (5.1, *6.0*)

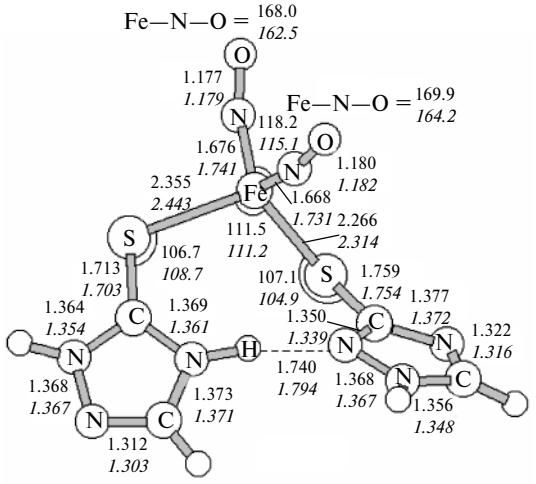

1e (7.4, *8.7*)

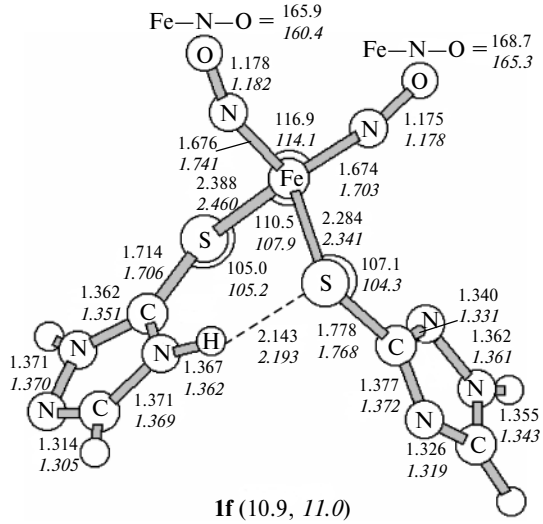

1f (10.9, *11.0*)

Fig. 1. Bond angles (in degrees), bond lengths (Å), and relative energies (kcal mol^{-1}, figures in parentheses) of complex **1a** and its isomers **1b**—**f** obtained from PBE and B3LYP (italicized) calculations.

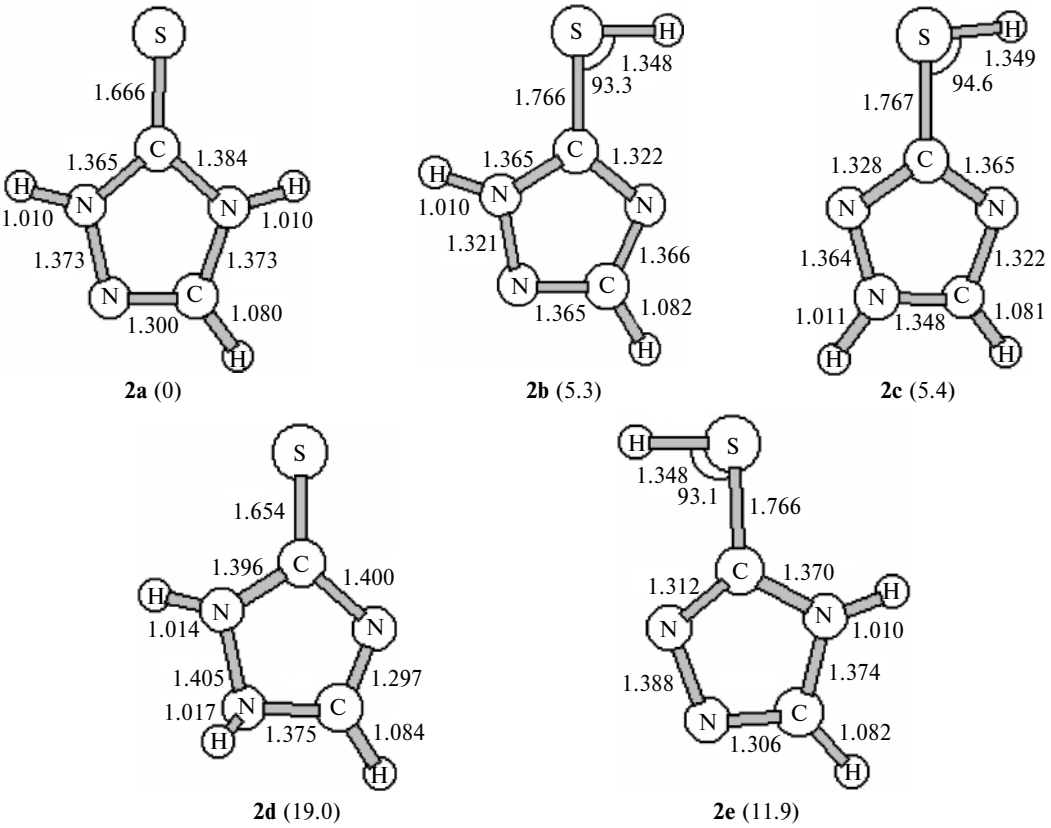

Fig. 2. Bond angles (in degrees) and bond lengths (Å) in isomeric forms of ligand **2a**—**e** obtained from B3LYP/6-31G* calculations. The B3LYP/6-311++G** calculated relative energies (in kcal mol^{-1}) are given in parentheses.

Table 2. Characteristics[a] of the electronic structure of complex **1**

Spin	E /kcal mol^{-1}	Fe		N(9)O(1)		N(10)O(2)		$<S^2>^b$
		q	SD	$-q$	SD	$-q$	SD	
				Experiment[12]				
		0.62		0.25		0.37		
				B3LYP/6-31G* calculations				
1/2	0	0.84	3.23	0.27	−1.19	0.28	−1.21	2.53 (5.06)
3/2	30.6	0.87	3.35	0.27	−1.18	0.31	0.62	4.85 (4.34)
5/2	59.6	0.88	3.27	0.24	0.04	0.31	1.44	8.86 (8.75)
				PBE/SBK calculations				
1/2	0	0.60	1.63	0.23	−0.44	0.26	−0.45	
3/2	39.4	0.65	2.01	0.26	0.17	0.29	0.27	
	27.8 [c]	0.62	2.22	0.27	−0.06	0.27	0.48	
5/2	80.5	0.78	2.75	0.29	0.44	0.36	1.25	
	47.9 [c]	0.67	2.94	0.21	0.11	0.34	1.50	

[a] Listed are the energies (E), charges (q), and spin densities (SD).
[b] Figures in parentheses denote the results obtained after projection.
[c] With allowance for system´s relaxation upon electron unpairing.

non-integer due to MO delocalization. This spin density distribution in the complex to a good accuracy corresponds to the one-determinant wave function $[d_1\alpha d_2\alpha d_3\alpha\pi_a\beta\pi_b\beta]$, where d_i are the orbitals mainly localized on the iron atom and π_a and π_b are the orbitals localized on different NO groups. This wave function is not an eigenfunction of

the S^2 operator because it contains all components with $S = 1/2$, 3/2, and 5/2. Therefore, the average squared spin S^2 for this wave function differs from the theoretical value for the doublet and equals 2.75. The $S = 5/2$ component contributes largely, because application of the projector, which "cuts" the $S = 3/2$ component, causes the average squared spin S^2 to become equal to 5.36. These values are in good agreement with the results of calculations (2.53 and 5.06, respectively, see Table 2)*. The true wave function of the complex should be an eigenfunction of the S^2 operator with an eigenvalue of 0.75. Since the system with five unpaired electrons allows a number of doublet states to be formed, projection of this one-determinant state on the state with the correct spin symmetry should be performed with inclusion of strong correlation of d-electron spins on the Fe atom due to Hund´s rule. This situation corresponds to formation of homeopolar bonds Fe—NO, which is not accompanied by significant changes in the electron configuration of the Fe atom.[17] Large S^2 value indicates strong mixing with the $S = 3/2$ and $S = 5/2$ states in the one-determinant ground-state wave function. Therefore, geometry optimization in the one-determinant approximation is in fact energy optimization for a superposition of the true states $S = 1/2$, $S = 3/2$, and $S = 5/2$ with corresponding statistical weights and unavoidably causes artifacts. In particular, this seems to be responsible for the longer B3LYP calculated N—O and Fe—N bond lengths compared to the corresponding experimental values. According to PBE calculations, the Fe—N bond lengths are similar to experimental ones, which is likely due to the weaker mixing with the spin states $S = 3/2$ and $S = 5/2$, and the spin densities on the Fe atom and NO ligands are lower. A similar effect, *i.e.*, influence of the mixing of higher-multiplicity states on the geometry of mononuclear anionic dinitrosyl iron complexes was reported in another study.[15] Table 2 lists the calculated charges and spin densities on the Fe atom and NO ligands in complex **1** in different spin states. The charges on the Fe atom and NO ligands are almost independent of system´s multiplicity. For the ground-state structure the Mulliken charges obtained from the B3LYP and PBE calculations are in reasonable agreement with the results of analysis of the exact electron density.[12]

The lower-lying states of multiplicity 3/2 and 5/2 correspond to successive spin flips in the NO groups (see Table 2). For the sextet state the average S^2 value is quite similar to a theoretical value of 8.75 for the $[d_1\alpha d_2\alpha d_3\alpha\pi_a\alpha\pi_b\alpha]$ wave function corresponding to the parallel orientation of the 3/2 spin of the Fe atom and the 1/2 spins of the NO ligands. At the same time the $S = 5/2$ state can be treated as formed from two triplet states, $[d_1\alpha\pi_a\alpha]$ and $[d_2\alpha\pi_b\alpha]$, and a doublet state for the remaining free d-electron in the atom. Then, it becomes evident that the corresponding Fe—N bonds formed involving the overlapping orbital pairs ($d_1\pi_a$ and $d_2\pi_b$) are cleaved, which leads to elongation of the Fe—N distances upon geometry optimization (see Table 1). This again indicates that the doublet ground state is formed involving the spin states $S = 3/2$ for the Fe atom and $S = 1/2$ for the NO ligands.

Changes in the geometry of the complex in the PBE-optimized structures of different multiplicity are summarized in Table 1. To a rough approximation, the changes in energy upon an increase in the spin of the complex by unity can be considered equal to the NO binding energy, namely, 30 (B3LYP) and 39 (PBE) kcal mol^{-1}. In the latter case the inclusion of system´s relaxation causes the energy expenditure to decrease to 28 kcal mol^{-1}. These energy differences are small, being comparable or smaller than typical binding energies of neutral ligands to unoccupied coordination sites. Therefore, one can expect that replacement of the NO ligand by the solvent molecule will be similar to a thermally neutral process.* The energy expenditure for simultaneous flip of two spins of the NO groups is nearly twice as large. However, noteworthy is that the doubled spin is mainly localized on one NO group to which partial electron density transfer from the second group occurs. In this respect, one ligand becomes more while the other ligand less electrophilic in spite of very similar Fe—NO distances. This qualitative distinction between the electronic structures of the NO ligands is in agreement with the observed[12] qualitative differences between the deformation electron density distribution around the two Fe—NO fragments, being a probable reason for large splitting of the NO vibrational frequencies (see below).

Figure 3 shows the experimental and theoretical IR spectra of complex **1** and Table 3 presents the assignment of spectral lines. The N—O stretching vibrations of the complex show good correspondence with those of the $Fe(NO)_2$ (1731.6, 1798.1 cm^{-1}) and $Fe(NO)_3$ (1742.6, 1794.6 cm^{-1}) species in low-temperature matrices.[18] The lines corresponding to the in-phase and out-of-phase NO vibrations are the most intense. Their experimental and theoretical intensities are similar. Theory also correctly reproduces a rather large splitting between the lines of the two NO ligands having almost identical coordination. However, the third intense line matching the line at 1725 cm^{-1} is absent in the theoretical spectra. Probably, this satellite line should be attributed to a product of

* Correspondence for the S^2 value indicates that the interpretation[15,16] of the electronic structure of dinitrosyl iron complexes as formed by the interaction of the spins of two NO^- ligands (1) with the spin of the Fe^{3+} ion (5/2) is somewhat incorrect.

* B3LYP calculations of the binding energy of the NO ligand gave a value of 29.3 kcal mol^{-1} and nearly zero energy for the reaction of NO replacement by H_2O.

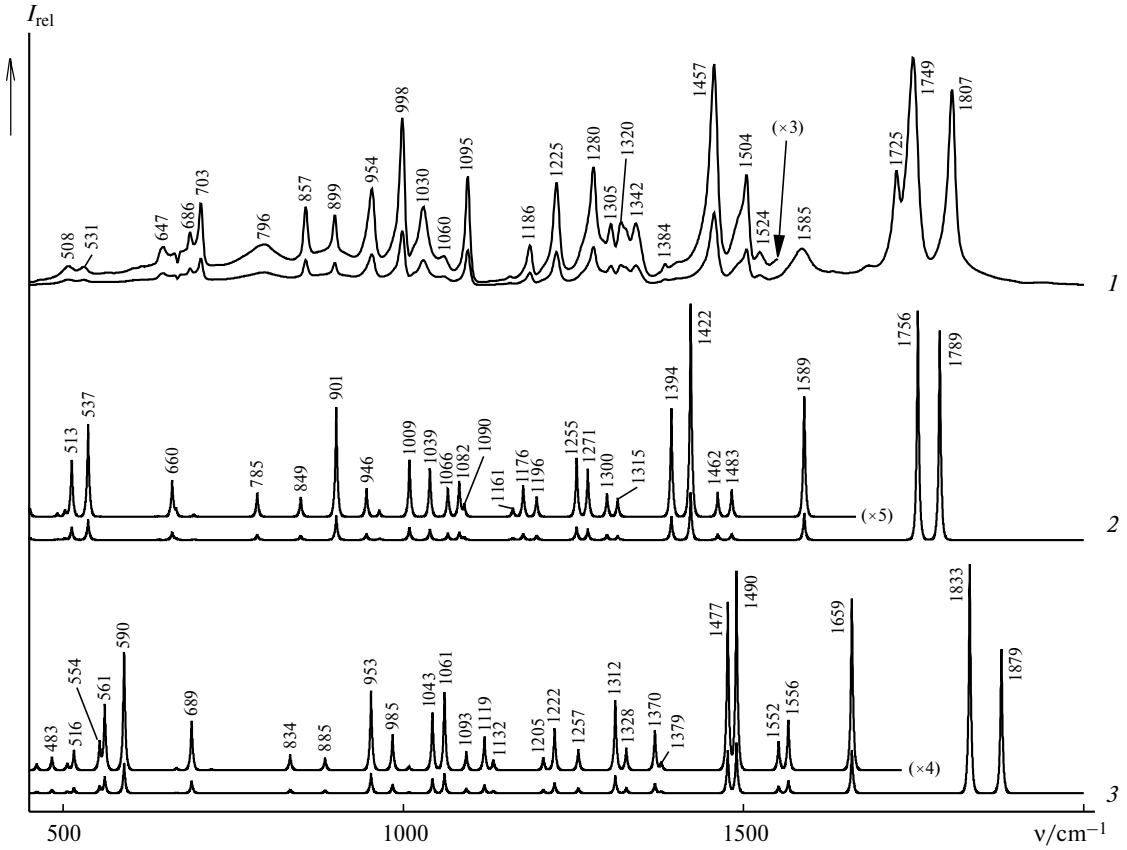

Fig. 3. IR spectra of complex **1**: experimental (with subtracted background) (*1*) and theoretical ones calculated by the PBE (*2*) and B3LYP (*3*) methods. Theoretical spectra were constructed using Lorentzian lines with a half-width of 2 cm^{-1}. For better resolution of the key lines the spectral region below 1720 cm^{-1} also shows the scaled spectra.

partial decomposition of complex **1** with the loss of one NO ligand. By and large the theoretical spectra provide a good idea of the structure of the experimental spectrum, the PBE method better reproducing positions of spectral lines and the B3LYP method giving more correct line intensities. This is particularly important for assignment of the lines at 647 and 686 cm^{-1}. The PBE calculated spectrum shows only three sufficiently intense lines in the region below 710 cm^{-1}. The spectrum obtained from B3LYP calculations exhibits additional lines, but all of them are below 600 cm^{-1}. These lines correspond to Fe—N vibrations; in contrast to other lines, their relative positions depend on the computational method used. It is the PBE method more correctly reproducing line positions that places these vibrations in the spectral region near 700 cm^{-1}. Noteworthy is the large width of the line at 1585 cm^{-1}. According to calculations, this line should be attributed to bending vibrations of the N(1)—H(1) bond, accompanied by changes in the length of the H(1)—N(6) hydrogen bond. This is just the reason for the line broadening. Some contribution of the N(1)—H(1) vibrations also causes broadening of the lines at 1504 cm^{-1}. In addition, the spectrum also shows a broad line at 796 cm^{-1}. In the region below 1000 cm^{-1} the theoretical spectra exhibit only one vibration at 953 (B3LYP) or 901 cm^{-1} (PBE), which is also accompanied by changes in the length of the H(1)—N(6) hydrogen bond. With allowance for possible influence of the packing effects we attributed this vibration based on its width rather than one-to-one correspondence between the experimental and theoretical spectra. The strong intramolecular hydrogen bond particularly manifests itself at frequencies higher than 2000 cm^{-1}, where a very broad band at 2100—2600 cm^{-1} with a local maximum at 2440 cm^{-1} is observed. According to calculations, it is this spectral region that corresponds to the N(1)—H(1) stretching vibration at a reduced frequency. An interesting feature of the theoretical spectra is almost complete degeneration of S—C vibrations that are too weak to be observed, despite some differences between the S—C bond lengths. This is consistent with the results of analysis of the electron density distribution for complex **1** in the crystalline state, which indicated an identical character of the deformation electron density for both S—C fragments.[12]

Thus, our theoretical study showed that the density functional methods correctly describe the structure

Table 3. Band assignment in the IR spectra of complex **1**

ν_{exp} /cm^{-1}	B3LYP/6-31G*		PBE/SBK		Assignment
	ν	μ	ν	μ	
2440	2684	1.13	2182	1.20	N(1)—H(1) stretching
1807	1879	14.7	1789	14.7	NO in-phase
1749	1832	14.8	1756	14.7	NO antiphase
1585	1659	1.65	1589	1.45	N(1)—H(1) bending
1504	1566	3.81	1483	3.83	N(3)—C(2)—N(2) bending + N(1)—H(1) bending
1504 sh	1552	3.19	1462	2.81	N(6)—C(5)—N(8) bending + N(7)—H(7) bending
1457	1490	2.19	1422	2.45	H(3)—N(3) bending + S(1)—C(1) stretching
1384	1477	2.92	1394	2.90	C(4)—N(7) stretching + N(7)—H(7) bending
1342	1379	5.29	1315	5.12	N(3)—C(1)—N(1) bending + C(2)—N(2) stretching
1320	1370	9.37	1300	9.54	C(4)—N(6) stretching + N(8)—C(5) stretching
1305	1328	3.11	1271	3.8	C(1)—N(1) stretching + N(3)—C(2) in-phase stretching + + H(2)—C(2) bending
1280	1312	2.97	1255	3.49	C(4)—N(6)—C(5) bending + N(7)—N(8)—C(5) bending + C(5)—H(5) bending
1225	1257	1.85	1196	1.96	N(7)—H(7) bending + C(4)—N(7) stretching
1186	1222	1.95	1176	2.07	C(2)—H(2) bending + N(3)—C(1) stretching
	1206	2.66	1161	2.41	C(5)—H(5) bending + N(6)—C(5) stretching
1065	1132	1.62	1090	2.05	N(3)—H(3) bending + N(1)—N(2) stretching
1065	1119	3.48	1082	3.35	N(7)—N(8) stretching
1060	1093	2.79	1066	2.23	N(1)—H(1) out-of-plane bending (H(3)—N(3)—C(2) bending + H(2)—C(2)—N(2) in-phase bending)
1030	1061	1.19	1039	2.16	N(1)—N(2) + N(1)—H(1) out-of-plane bending
998	1043	4.96	1009	5.56	C(5)—N(6)—C(4) + N(6)—C(4)—N(7) out-of-phase
	1008	5.82	965	6.16	C(1)—N(3)—C(2) + N(3)—C(2)—N(2) out-of-phase (N(3)—C(1)—N(7) bending)
954	984	4.45	946	6.09	C(5)—N(8)—N(7) bending
899	953	5.84	901	5.04	C(2)—N(2)—N(1) bending + H(1)...N(6) stretching
857	885	1.35	849	1.33	C(5)—H(5) out-of-plane bending
796	834	1.34	785	1.34	C(2)—H(2) out-of-plane bending
	718	5.21	692	5.46	N(6)—C(4)—N(7) out-of-plane bending
	461	14.7	666	14.9	Fe—N—O bending in N—Fe—N plane, in-phase
703	689	2.77	660	3.16	C(5)—N(8)—N(7) out-of-plane bending
	687	5.40	656	3.59	N(3)—C(1)—N(1) + N(3)—C(2)—N(2) bending in nonplanar phase (N(3)—C(1)—N(1))
	667	3.20	643	5.44	C(2)—N(2)—N(1) out-of-plane bending
686	554	20.7	639	20.6	Fe—N antiphase
647	484	20.3	554	18.4	Fe—N in-phase
531	590	1.44	537	1.38	H(3)—N(3) out-of-plane bending
508	561	1.54	513	1.45	N(7)—H(7) out-of-plane bending
	516	15.0	503	13.8	S(1)—C(2) stretching
	506	16.5	492	14.3	S(2)—C(4) stretching
	338	16.1	451	15.7	Fe—N—O bending in-phase normal to N—Fe—N plane
	285	11.5	387	13.7	Fe—N—O bending antiphase normal to N—Fe—N plane
	185	8.95	245	11.8	Fe—N—O bending antiphase in N—Fe—N plane

* Frequencies are given in cm^{-1} and the effective masses μ are given in a.m.u. For different eigenvectors of vibrations, the figures in parentheses correspond to B3LYP calculations.

and IR spectra of the neutral mononuclear nitrosyl iron complex $[Fe(SC_2H_3N_3)(SC_2H_2N_3)(NO)_2]$. This made it possible to correlate IR bands with normal vibrations of the complex and to reveal the presence of an impurity, which is probably formed as a result of partial decomposition of the complex with the loss of one NO ligand. Analysis of the electronic structure of the complex indicates that the ground state with $S = 1/2$ is formed upon pairing of electrons of the iron ion with the electron configuration d^7 ($S = 3/2$) with the unpaired electrons of the NO ligands. As a result the Fe^+ ion forms two homeopolar bonds Fe—NO and the state of the Fe atom in the complex can be treated as effective Fe^{III} state.

This work was financially supported by the Council on Grants at the President of the Russian Federation (Program of the State Support of Leading Scientific Schools in Russia, Grant NSh-4525.2006.3) and partially supported by the Russian Foundation for Basic Research (Grant 06-03-32381-a).

References

1. A. R. Butler and I. L. Megson, *Chem. Rev.*, 2002, **102**, 155.
2. V. G. Granik and N. B. Grigor´ev, *Izv. Akad. Nauk. Ser. Khim.*, 2002, 1268 [*Russ. Chem. Bull., Int. Ed.*, 2002, **51**, 1375].
3. V. G. Granik and N. B. Grigor´ev, *Oksid Azota (NO)* [*Nitrogen Monoxide*], Vuz. Kniga, Moscow, 2004, Sect. II (in Russian).
4. H. Strasdeit, B. Krebs, and G. Henkel, *Z. Naturforsch.*, 1986, **41B**, 1357.
5. K. M. Bultusis, K. D. Karlin, H. N. Rabinowitz, J. C. Dewan, and S. J. Lippard, *Inorg. Chem.*, 1980, **19**, 2627.
6. Ch.-Yi Chiang, M. L. Miller, J. H. Reibenspies, and M. Y. Darenbourg, *J. Am. Chem. Soc.*, 2004, **126**, 10867.
7. T. C. Harrop, D. Song, and S. Lippard, *J. Am. Chem. Soc.*, 2006, **128**, 3528.
8. F.-T. Tsai, S.-J. Chiou, M.-C. Tsai, M.-L. Tsai, H.-W. Huang, M.-H. Chiang, and W.-F. Liaw, *Inorg. Chem.*, 2005, **44**, 5872.
9. Ch. M. Menzies an P. J. Squattrito, *Inorg. Chim. Acta*, 2001, **314**, 194.
10. S. A. Goncharova, T. A. Raevskaya, N. P. Konovalova, and V. T. Kagiya, *Voprosy Onkologii*, 2000, **46**, 202 [*Problems in Oncology*, 2000, **46** (Engl. Transl.)]; S. N. Senapatu, *11th Ann. Meeting of Japanese Society of Therapeutic Radiation Oncology (JASTRO) (Maebashi, Gunma, Japan, November 21, 1998)*, Machashi, 1998.
11. N. A. Sanina, O. A. Rakova, S. M. Aldoshin, G. V. Shilov, Yu. M. Shulga, A. V. Kulikov, and N. S. Ovanesyan, *Mendeleev Commun.*, 2004, **1**, 9.
12. N. A. Sanina and S. M. Aldoshin, *Tez. dokl. XXIII Mezhd. Chugaevskoj konferentsii po koordinatsionnoj khimii (4—7 Sentyabrya 2007, Odessa)* [*Abstrs XXIII Int. Chugaev Conf. on Coord. Chem.*], Kiev, 2007, 225.
13. M. J. Frisch, G. W. Trucks, H. B. Schlegel, G. E. Scuseria, M. A. Robb, J. R. Cheeseman, V. G. Zakrzewski, J. A. Montgomery, Jr., R. E. Stratmann, J. C. Burant, S. Dapprich, J. M. Millam, A. D. Daniels, K. N. Kudin, M. C. Strain, O. Farkas, J. Tomasi, V. Barone, M. Cossi, R. Cammi, B. Mennucci, C. Pomelli, C. Adamo, S. Clifford, J. Ochterski, G. A. Petersson, P. Y. Ayala, Q. Cui, K. Morokuma, D. K. Malick, A. D. Rabuck, K. Raghavachari, J. B. Foresman, J. Cioslowski, J. V. Ortiz, A. G. Baboul, B. B. Stefanov, G. Liu, A. Liashenko, P. Piskorz, I. Komaromi, R. Gomperts, R. L. Martin, D. J. Fox, T. Keith, M. A. Al-Laham, C. Y. Peng, A. Nanayakkara, C. Gonzalez, M. Challacombe, P. M. W. Gill, B. Johnson, W. Chen, M. W. Wong, J. L. Andres, C. Gonzalez, M. Head-Gordon, E. S. Replogle, and J. A. Pople, *GAUSSIAN 98*, *Revision A.7*, Gaussian, Inc., Pittsburgh (PA), 1998.
14. D. N. Laikov, *Chem. Phys. Lett.*, 1997, **81**, 151.
15. M. Jaworska and Z. Stazicki, *J. Organomet. Chem.*, 2004, **689**, 1702.
16. M. Jaworska and Z. Stazicki, *New J. Chem.*, 2005, **29**, 604.
17. A. F. Shestakov, Yu. N. Shul´ga, N. S. Emel´yanova, N. A. Sanina, and S. M. Aldoshin, *Izv. Akad. Nauk*, *Ser. Khim.*, 2006, 2053 [*Russ. Chem. Bull., Int. Ed.*, 2006, **55**, 2143].
18. L. Andrew and A. Citra, *Chem. Rev.*, 2002, **102**, 885.

Received December 29, 2006;
in revised form March 15, 2007